# Resolved Momentum Control: Humanoid Motion Planning Based on the Linear and Angular Momentum

**Conference Paper** · November 2003

DOI: 10.1109/IROS.2003.1248880 · Source: IEEE Xplore



**7 authors**, including:

Shuuji Kajita
National Institute of Advanced Industrial Science and Technology
**217** PUBLICATIONS **15,171** CITATIONS
SEE PROFILE

Fumio Kanehiro
National Institute of Advanced Industrial Science and Technology
**266** PUBLICATIONS **12,909** CITATIONS
SEE PROFILE

Kiyoshi Fujiwara
National Institute of Advanced Industrial Science and Technology
**87** PUBLICATIONS **5,135** CITATIONS
SEE PROFILE

Kensuke Harada
Graduate School of Engineering Science, Osaka University
**484** PUBLICATIONS **8,857** CITATIONS
SEE PROFILE

Proceedings of the 2003 IEEE/RSJ
Intl. Conference on Intelligent Robots and Systems
Las Vegas, Nevada · October 200303

# Resolved Momentum Control: Humanoid Motion Planning based on the Linear and Angular Momentum

Shuuji KAJITA, Fumio KANEHIRO, Kenji KANEKO, Kiyoshi FUJIWARA,
Kensuke HARADA, Kazuhito YOKOI and Hirohisa HIRUKAWA

National Institute of Advanced Industrial Science and Technology (AIST)
Tsukuba Central 2, 1-1-1 Umezono, Tsukuba, Ibaraki, 305-8568 Japan
E-mail: {s.kajita,f-kanehiro,k.kaneko,k-fujiwara,
kensuke.harada,kazuhito.yokoi,hiro.hirukawa}@aist.go.jp

## Abstract

*We introduce a method to generate whole body motion of a humanoid robot such that the resulted total linear/angular momenta become specified values. First, we derive a linear equation which gives the total momentum of a robot from its physical parameters, the base link speed and the joint speeds. Constraints between the legs and the environment are also considered. The whole body motion is calculated from a given momentum reference by using a pseudo-inverse of the inertia matrix. As examples, we generated the kicking and walking motions and tested on the actual humanoid robot HRP-2. This method, the Resolved Momentum Control, gives us a unified framework to generate various maneuver of humanoid robots.*

## 1 Introduction

Smooth and dexterous control of complicated mechanisms is an important subject of robotics. Humanoid robots can be regarded as its ultimate goal, and recent development of reliable biped walking gives ordinally people even an *illusion* of a perfect multi-purpose machine [1, 2, 3, 4, 5]. However, once we step out the field of walking control, humanoid robots can perform very limited tasks. Although we can program our robot for a particular purpose, we can't do that for thousands of tasks in thousands of different environments as humanoid robots encounter in real world. Here we have a problem.

As one of the possible solutions, Wooten and Hodgins showed their simulated human model can perform various dynamic motions including inward/backward somersault, back handspring, vertical leap, broad jump and so on. To generate them, they combined four basic behaviors, which are leaping, tumbling, landing and balancing [6].

In this paper, to establish a unified framework producing variety of motion, we rely on the basic law of physics, an equation of motion written with momentum. No matter how a robot has complicated structure, we can determine its total linear and angular momenta. The total momentum is a vector of six elements, which describes macroscopic behavior of the entire robot. Since the momentum vector has a linear relationship with the joint speed vector, we can calculate joint speeds which will realize the desired momentum. With this strategy, it is shown that we can easily generate a humanoid's balancing, walking and other motions.

This paper is organized as follows. In Section 2, we describe basic equations of momentum calculation. Using the equations, we show a method of motion planning and name it the Resolved Momentum Control in Section 3. At the end of Section 3, we discuss the relationship between our resolved momentum control and other conventional methods. In Section 4, we explain the detailed calculation of inertia matrix which is necessary to our method. In Section 5, using a humanoid robot HRP-2, kicking and walking motions are generated and tested. Section 6 concludes the paper and states our future plan.

## 2 Momentum equation

### 2.1 Momentum and joint velocities

We represent a humanoid robot as a mechanism of tree structure whose root is a free-flying base link

(pelvis), a rigid body having 6 D.O.F in 3D space (Figure 1). We define the frame $\Sigma_B$ embedded in the base link whose translational velocity and angular velocity are $\boldsymbol{v}_B$ and $\boldsymbol{\omega}_B$, respectively. In addition, we define a $n \times 1$ column vector $\dot{\boldsymbol{\theta}}$ which contains velocities of all joints as its elements where $n$ is the total number of joints. The linear momentum $\boldsymbol{P}$ $(3 \times 1)$ and the angular momentum $\boldsymbol{L}$ $(3 \times 1)$ of the whole mechanism are given by

$$\begin{bmatrix} \boldsymbol{P} \\ \boldsymbol{L} \end{bmatrix} = \begin{bmatrix} \tilde{m}\boldsymbol{E} & -\tilde{m}\hat{\boldsymbol{r}}_{B\to\tilde{c}} & \boldsymbol{M}_{\dot{\theta}} \\ \boldsymbol{0} & \tilde{\boldsymbol{I}} & \boldsymbol{H}_{\dot{\theta}} \end{bmatrix} \begin{bmatrix} \boldsymbol{v}_B \\ \boldsymbol{\omega}_B \\ \dot{\boldsymbol{\theta}} \end{bmatrix} \quad (1)$$

where $\tilde{m}$ is the total mass of the robot, $\boldsymbol{E}$ is an identity matrix of $3\times3$, $\boldsymbol{r}_{B\to\tilde{c}}$ is the $3\times1$ vector from the base link to the total center of mass (CoM) and $\tilde{\boldsymbol{I}}$ is the $3\times3$ inertia matrix with respect to the CoM. $\boldsymbol{M}_{\dot{\theta}}$ and $\boldsymbol{H}_{\dot{\theta}}$ are the $3 \times n$ inertia matrices which indicate how the joint speeds affect to the linear momentum and the angular momentum respectively. $\hat{}$ is an operator which translates a vector of $3\times1$ into a skew symmetric $3\times3$ matrix which is equivalent to a cross product.

In this paper, we assume all vectors of position, velocity and angular velocity are represented in the Cartesian frame $\Sigma_O$ fixed on the ground.

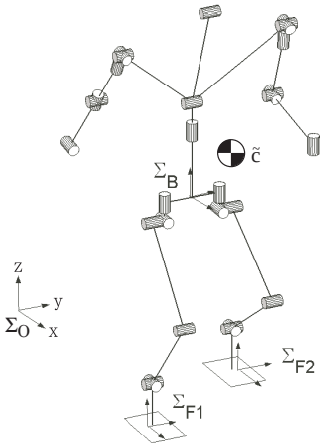


Figure 1: A model of humanoid robot

## 2.2 Constraints of foot contact

Equation (1) gives the total momentum of a flying robot. However, when the robot is in contact with the ground, we must take into account of constraints that reduce the total D.O.F of the system. The foot velocities $(\boldsymbol{v}_{F_i},\ \boldsymbol{\omega}_{F_i})$ of the frame $\Sigma_{F_i}(i = 1, 2)$ are given by

$$\begin{bmatrix} \boldsymbol{v}_{F_i} \\ \boldsymbol{\omega}_{F_i} \end{bmatrix} = \begin{bmatrix} \boldsymbol{E} & \hat{\boldsymbol{r}}_{B\to F_i} \\ \boldsymbol{0} & \boldsymbol{E} \end{bmatrix} \begin{bmatrix} \boldsymbol{v}_B \\ \boldsymbol{\omega}_B \end{bmatrix} + \boldsymbol{J}_{leg_i}\dot{\boldsymbol{\theta}}_{leg_i}, \quad (2)$$

where $\boldsymbol{J}_{leg_i}$ is a Jacobian matrix $(6 \times 6)$ calculated from the leg configuration, $\boldsymbol{r}_{B\to F_i}$ is a position vector $(3 \times 1)$ from the base frame to the foot frame and $\dot{\boldsymbol{\theta}}_{leg_i}$ is the joint speed vector $(6 \times 1)$ of each leg. If $\boldsymbol{J}_{leg_i}(i = 1, 2)$ are non singular, the vectors for the leg joint speeds are given by

$$\dot{\boldsymbol{\theta}}_{leg_i} = \boldsymbol{J}^{-1}_{leg_i} \begin{bmatrix} \boldsymbol{v}_{F_i} \\ \boldsymbol{\omega}_{F_i} \end{bmatrix} - \boldsymbol{J}^{-1}_{leg_i} \begin{bmatrix} \boldsymbol{E} & \hat{\boldsymbol{r}}_{B\to F_i} \\ \boldsymbol{0} & \boldsymbol{E} \end{bmatrix} \begin{bmatrix} \boldsymbol{v}_B \\ \boldsymbol{\omega}_B \end{bmatrix}. \quad (3)$$

Let us divide the whole joint speed vector into leg parts and the rest part as

$$\dot{\boldsymbol{\theta}} = [\dot{\boldsymbol{\theta}}^T_{leg_1} \quad \dot{\boldsymbol{\theta}}^T_{leg_2} \quad \dot{\boldsymbol{\theta}}^T_{free}]^T, \quad (4)$$

where $\dot{\boldsymbol{\theta}}_{free}$ is the joint speed for waist, arms and head. We also divide the corresponding inertia matrices as

$$\begin{aligned} \boldsymbol{M}_{\dot{\theta}} &= [\boldsymbol{M}_{leg_1}\ \boldsymbol{M}_{leg_2}\ \boldsymbol{M}_{free}], \\ \boldsymbol{H}_{\dot{\theta}} &= [\boldsymbol{H}_{leg_1}\ \boldsymbol{H}_{leg_2}\ \boldsymbol{H}_{free}]. \end{aligned}$$

Then, we can rewrite the momentum equation (1) as

$$\begin{aligned} \begin{bmatrix} \boldsymbol{P} \\ \boldsymbol{L} \end{bmatrix} &= \begin{bmatrix} \tilde{m}\boldsymbol{E} & -\tilde{m}\hat{\boldsymbol{r}}_{B\to\tilde{c}} \\ \boldsymbol{0} & \tilde{\boldsymbol{I}} \end{bmatrix} \begin{bmatrix} \boldsymbol{v}_B \\ \boldsymbol{\omega}_B \end{bmatrix} \\ &+ \sum_{i=1}^{2} \begin{bmatrix} \boldsymbol{M}_{leg_i} \\ \boldsymbol{H}_{leg_i} \end{bmatrix} \dot{\boldsymbol{\theta}}_{leg_i} + \begin{bmatrix} \boldsymbol{M}_{free} \\ \boldsymbol{H}_{free} \end{bmatrix} \dot{\boldsymbol{\theta}}_{free}. \end{aligned} \quad (5)$$

By substituting (3) into (5), we obtain the momentum equation under the constraint as

$$\begin{bmatrix} \boldsymbol{P} \\ \boldsymbol{L} \end{bmatrix} = \begin{bmatrix} \boldsymbol{M}^*_B & \boldsymbol{M}_{free} \\ \boldsymbol{H}^*_B & \boldsymbol{H}_{free} \end{bmatrix} \begin{bmatrix} \boldsymbol{\xi}_B \\ \dot{\boldsymbol{\theta}}_{free} \end{bmatrix} + \sum_{n=1}^{2} \begin{bmatrix} \boldsymbol{M}^*_{Fi} \\ \boldsymbol{H}^*_{Fi} \end{bmatrix} \boldsymbol{\xi}_{F_i}, \quad (6)$$

where

$$\begin{aligned} \boldsymbol{\xi}_B &\equiv [\boldsymbol{v}^T_B \quad \boldsymbol{\omega}^T_B]^T, \\ \boldsymbol{\xi}_{F_i} &\equiv [\boldsymbol{v}^T_{F_i} \quad \boldsymbol{\omega}^T_{F_i}]^T, \\ \begin{bmatrix} \boldsymbol{M}^*_B \\ \boldsymbol{H}^*_B \end{bmatrix} &\equiv \begin{bmatrix} \tilde{m}\boldsymbol{E} & -\tilde{m}\hat{\boldsymbol{r}}_{B\to c} \\ \boldsymbol{0} & \tilde{\boldsymbol{I}} \end{bmatrix} \\ &\quad - \sum_{n=1}^{2} \begin{bmatrix} \boldsymbol{M}^*_{Fi} \\ \boldsymbol{H}^*_{Fi} \end{bmatrix} \begin{bmatrix} \boldsymbol{E} & \hat{\boldsymbol{r}}_{B\to F_i} \\ \boldsymbol{0} & \boldsymbol{E} \end{bmatrix}, \\ \begin{bmatrix} \boldsymbol{M}^*_{Fi} \\ \boldsymbol{H}^*_{Fi} \end{bmatrix} &\equiv \begin{bmatrix} \boldsymbol{M}_{leg_i} \\ \boldsymbol{H}_{leg_i} \end{bmatrix} \boldsymbol{J}^{-1}_{leg_i}. \end{aligned}$$

The second term in the right hand side of (6) indicates the extra momentum generated by specifying the foot speed.

## 3 Resolved Momentum Control

### 3.1 Setting momentum reference

For every mechanical system, no matter how its structure or behavior is complicated, we can determine the position of the CoM $\tilde{\boldsymbol{c}}$, the linear momentum $\boldsymbol{P}$ and the angular momentum $\boldsymbol{L}$ for the total mechanism.

Dividing the total linear momentum $\boldsymbol{P}$ by the total mass $\tilde{m}$, we obtain the translational speed of the CoM.

$$\frac{d}{dt}\tilde{\boldsymbol{c}} = \frac{\boldsymbol{P}}{\tilde{m}} \tag{7}$$

Thus, we can control the position of the CoM by manipulating the linear momentum.

As the extension of this, we propose a method of control or pattern generation by manipulating the total (linear and angular) momentum. Let us call this method the *Resolved Momentum Control*. The reference motion of a humanoid robot can be specified by assuming a rigid body whose mass and moment of inertia are equal to the target. However, we cannot associate the orientation of this imaginary object to the robot, since a rigid body can not hold enough information to represent the internal structure of the multi-body system.

### 3.2 Momentum selection and control by pseudo-inverse

In many applications, we do not have to specify all six elements of the momentum. Moreover, in some case we encounters a numerical unstability by specifying the all elements of the reference momentum. Therefore, we introduce a selection matrix $\boldsymbol{S}$ which is $l\times 6$ ( $0 < l \leq 6$) to pick up the elements of the momentum to be controlled. The selection of the momentum is given by

$$\boldsymbol{S} \equiv \begin{bmatrix} \boldsymbol{e}_{s_1}^T \\ \vdots \\ \boldsymbol{e}_{s_l}^T \end{bmatrix}, \tag{8}$$

where $\boldsymbol{e}_{s_i}$ is a column vector of $6\times 1$ that has one at $s_i$-th row and zeros for the rest. $s_i$ specifies the element of the momentum we want to pick up. Transposing the second term of (6) from the right side to the left side, then multiplying $\boldsymbol{S}$ from left, we obtain the following equation.

$$\boldsymbol{y} = \boldsymbol{A}\begin{bmatrix} \boldsymbol{\xi}_B \\ \dot{\boldsymbol{\theta}}_{free} \end{bmatrix}, \tag{9}$$

where

$$\boldsymbol{y} \equiv \boldsymbol{S}\left\{ \begin{bmatrix} \boldsymbol{P}^{ref} \\ \boldsymbol{L}^{ref} \end{bmatrix} - \sum_{n=1}^{2} \begin{bmatrix} \boldsymbol{M}_{Fi}^{*} \\ \boldsymbol{H}_{Fi}^{*} \end{bmatrix} \boldsymbol{\xi}_{F_i}^{ref} \right\}, \tag{10}$$

$$\boldsymbol{A} \equiv \boldsymbol{S}\begin{bmatrix} \boldsymbol{M}_B^{*} & \boldsymbol{M}_{free} \\ \boldsymbol{H}_B^{*} & \boldsymbol{H}_{free} \end{bmatrix}. \tag{11}$$

Here $\boldsymbol{P}^{ref}$ is the reference linear momentum, $\boldsymbol{L}^{ref}$ is the reference angular momentum and $\boldsymbol{\xi}_{F_i}^{ref}$ is the reference velocity for each foot.

Using (9), the target speed which realizes the reference momentum and the speed $(\boldsymbol{\xi}_B^{ref}, \dot{\boldsymbol{\theta}}^{ref})$ is calculated as the least square solution by

$$\begin{bmatrix} \boldsymbol{\xi}_B \\ \dot{\boldsymbol{\theta}}_{free} \end{bmatrix} = \boldsymbol{A}^{\dagger}\boldsymbol{y} + (\boldsymbol{E} - \boldsymbol{A}^{\dagger}\boldsymbol{A}) \begin{bmatrix} \boldsymbol{\xi}_B^{ref} \\ \dot{\boldsymbol{\theta}}_{free}^{ref} \end{bmatrix}, \tag{12}$$

where $\boldsymbol{A}^{\dagger}$ is a pseudo-inverse (the least-squares inverse) of $\boldsymbol{A}$. This equation gives the Resolved Momentum Control.

### 3.3 Related works

The resolved momentum control can be regarded as a unified scheme of conventional methods for humanoid robots. Kagami et al. [7] proposed a balance control of a humanoid by manipulating the CoM with second order nonlinear programming optimization. Sugihara et al. proposed a balancing and walking controller based on the CoM manipulation [8]. Both methods mainly take into account of linear momentum control. Especially, their *COG Jacobian* [7, 8] can be obtained when we divided the matrices $\boldsymbol{M}_B^{*}$ and $\boldsymbol{M}_{free}$ of (6) by the total mass $\tilde{m}$.

Baerlocher and Boulic discussed the control of highly redundant mechanical system under the multiple demands like reaching target, obstacle avoidance and balancing [9]. They encoded the task priority by using pseudo-inverse and the damped least-squares inverse. By combining the Resolved Momentum Control, we can extend their method for a dynamic motion.

In space robotics, many researchers have already pointed out the importance of the total momentum. Umetani and Yoshida discussed a control of free flying robot equipped with a manipulator and proposed a resolved motion rate control combined with the momentum conservation [10]. An equivalent calculation is possible using our resolved momentum control. Let us assume a space robot equipped with *one leg* orbiting in space. We set the reference momentum as

$\boldsymbol{P}^{ref} = \boldsymbol{0}, \boldsymbol{L}^{ref} = \boldsymbol{0}$ taking adequate reference frame. By using a selection matrix $\boldsymbol{S} = \boldsymbol{E}$, (10) becomes

$$\boldsymbol{y} = \left\{ \begin{bmatrix} \boldsymbol{0} \\ \boldsymbol{0} \end{bmatrix} - \begin{bmatrix} \boldsymbol{M}^*_{F_1} \\ \boldsymbol{H}^*_{F_1} \end{bmatrix} \boldsymbol{\xi}^{ref}_{F_1} \right\},$$

where $\boldsymbol{\xi}^{ref}_{F_1}$ is the desired foot speed in space. For a space robot with one leg of 6 D.O.F, matrix $\boldsymbol{A}$ of (11) becomes square. Therefore, (12) is

$$\boldsymbol{\xi}_B = \boldsymbol{A}^{-1}\boldsymbol{y},$$

where $\boldsymbol{\xi}_B$ is the base link speed obtained by the reaction of the leg motion. Finally, the joint speed is given by the following equation (same as (3)).

$$\dot{\boldsymbol{\theta}}_{leg_1} = \boldsymbol{J}^{-1}_{leg_1} \left( \boldsymbol{\xi}^{ref}_{F_1} - \begin{bmatrix} \boldsymbol{E} & \hat{\boldsymbol{r}}_{B\to F_1} \\ \boldsymbol{0} & \boldsymbol{E} \end{bmatrix} \boldsymbol{\xi}_B \right)$$

## 4 Calculation of the inertia matrices

In this section we describe a method to calculate the inertia matrices $\boldsymbol{M}_{\dot{\theta}}$ and $\boldsymbol{H}_{\dot{\theta}}$, which appears in (1).

Figure 2 shows a part of the robot links containing the joint $j-1$ and joint $j$. We assume the robot can rotate its joints with specified speed under the proper control law like PD feedback. The joint $j$'s rotation with speed $\dot{\theta}_j$ yields additional linear and angular momenta of

$$\begin{aligned} \boldsymbol{P}_j &= \boldsymbol{\omega}_j \times (\tilde{\boldsymbol{c}}_j - \boldsymbol{r}_j)\tilde{m}_j, && (13) \\ \boldsymbol{L}_j &= \tilde{\boldsymbol{c}}_j \times \boldsymbol{P}_j + \tilde{\boldsymbol{I}}_j \boldsymbol{\omega}_j, && (14) \\ \boldsymbol{\omega}_j &\equiv \boldsymbol{a}_j \dot{\theta}_j, && (15) \end{aligned}$$

where $\boldsymbol{r}_j$ and $\boldsymbol{a}_j$ are the position vector and the rotation axis vector of the joint $j$. $\tilde{m}_j$, $\tilde{c}_j$ and $\tilde{\boldsymbol{I}}_j$ mean mass, center of mass and inertia tensor of all link structure driven by the joint $j$.

Now, the columns of the inertia matrices corresponding to the joint $j$ are determined by the following equations

$$\begin{aligned} \boldsymbol{m}_j &\equiv \boldsymbol{P}_j / \dot{\theta}_j, && (16) \\ \boldsymbol{h}_j &\equiv \boldsymbol{L}_j / \dot{\theta}_j, && (17) \end{aligned}$$

where $\boldsymbol{m}_j$ and $\boldsymbol{h}_j$ are vectors of $3 \times 1$. By comparing (13) and (16), we obtain $\boldsymbol{m}_j$. Likewise, by comparing (14) and (17), we obtain $\boldsymbol{h}_j$ by

$$\begin{aligned} \boldsymbol{m}_j &= \boldsymbol{a}_j \times (\tilde{\boldsymbol{c}}_j - \boldsymbol{r}_j)\tilde{m}_j, && (18) \\ \boldsymbol{h}_j &= \tilde{\boldsymbol{c}}_j \times \boldsymbol{m}_j + \tilde{\boldsymbol{I}}_j \boldsymbol{a}_j. && (19) \end{aligned}$$

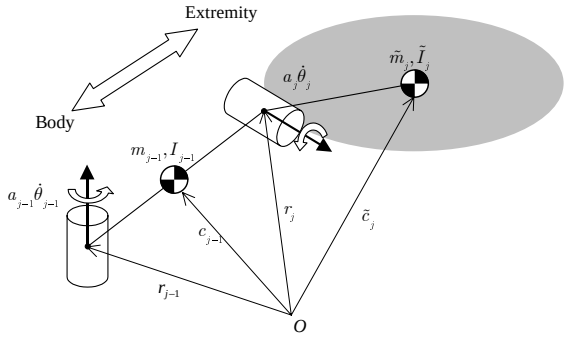


Figure 2: Link configulation

Using these column vectors, the inertia matrices $\boldsymbol{M}_{\dot{\theta}}$ and $\boldsymbol{H}_{\dot{\theta}}$ are constructed like

$$\begin{aligned} \boldsymbol{M}_{\dot{\theta}} &= [\boldsymbol{m}_1, \boldsymbol{m}_2, \dots \boldsymbol{m}_n], && (20) \\ \boldsymbol{H}_{\dot{\theta}} &= {}^0\boldsymbol{H}_{\dot{\theta}} - \widehat{\tilde{\boldsymbol{c}}}\, \boldsymbol{M}_{\dot{\theta}}, && (21) \\ {}^0\boldsymbol{H}_{\dot{\theta}} &\equiv [\boldsymbol{h}_1, \boldsymbol{h}_2, \dots \boldsymbol{h}_n]. && (22) \end{aligned}$$

Equation (21) converts the angular momentum about the ground frame into the angular momentum about the robot's CoM.

We can calculate $\tilde{m}_j$, $\tilde{\boldsymbol{c}}_j$ and $\tilde{\boldsymbol{I}}_j$ from an extremity to the body side by using a recursive algorithm. Assuming we have already calculated $\tilde{m}_j$, $\tilde{\boldsymbol{c}}_j$ and $\tilde{\boldsymbol{I}}_j$ about joint $j$, the parameters of adjacent joint $j-1$ can be calculated as

$$\begin{aligned} \tilde{m}_{j-1} &= \tilde{m}_j + m_{j-1}, && (23) \\ \tilde{\boldsymbol{c}}_{j-1} &= (\tilde{m}_j \tilde{\boldsymbol{c}}_j + m_{j-1}\boldsymbol{c}_{j-1})/(\tilde{m}_j + m_{j-1}), && (24) \\ \tilde{\boldsymbol{I}}_{j-1} &= \tilde{\boldsymbol{I}}_j + \tilde{m}_j D(\tilde{\boldsymbol{c}}_j - \tilde{\boldsymbol{c}}_{j-1}) + \boldsymbol{R}_{j-1}\boldsymbol{I}_{j-1}\boldsymbol{R}^T_{j-1} \\ &\quad + m_{j-1} D(\boldsymbol{c}_{j-1} - \tilde{\boldsymbol{c}}_{j-1}), && (25) \\ D(r) &\equiv \hat{\boldsymbol{r}}^T \hat{\boldsymbol{r}}, && (26) \end{aligned}$$

where $\boldsymbol{R}_{j-1}$, $m_{j-1}$ and $\boldsymbol{I}_{j-1}$ are $3 \times 3$ orientation matrix, mass and inertia tensor around the center of the $j-1$ th link, respectively.

## 5 Examples

### 5.1 Kick motion

In this section we evaluate the motion generated by the Resolved Momentum Control using an actual humanoid robot HRP-2[11]. HRP-2 is a humanoid robot of 154cm height and weighs 58kg developed in Humanoid Robotics Project (HRP) of METI [12].

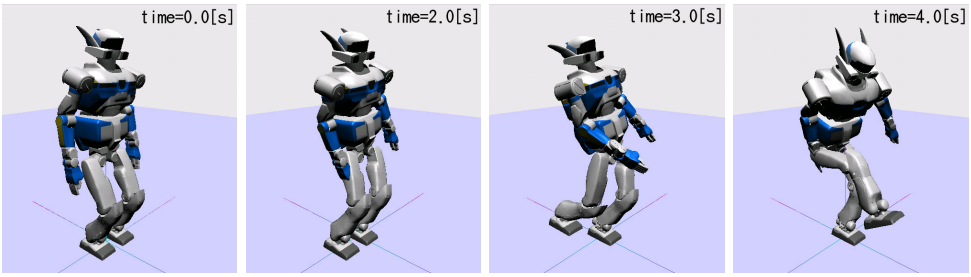


Figure 3: Kick: $S = E$

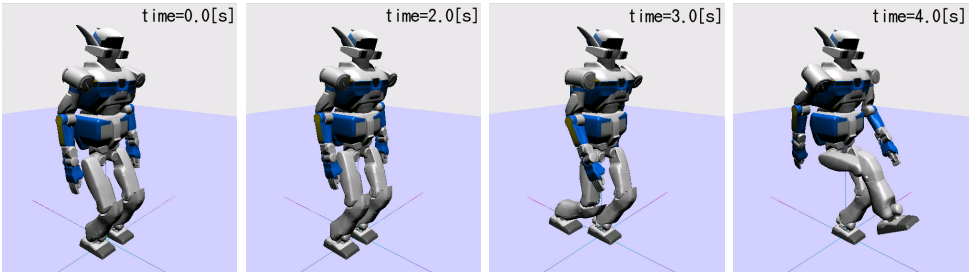


Figure 4: Kick: $S = [\boldsymbol{e}_1\boldsymbol{e}_2\boldsymbol{e}_3\boldsymbol{e}_6]^T$

Figures 3 and 4 show the calculated kicking action of HRP-2. The target momentum was given such that the robot's CoM follows given references by

$$P_{x,y}^{ref} = \tilde{m}K_p(\tilde{c}_{x,y}^{ref} - \tilde{c}_{x,y}) + \dot{\tilde{c}}_{x,y}^{ref}, \quad (27)$$

$$P_z^{ref} = \tilde{m}K_p(z_B^{ref} - z_B), \quad (28)$$

$$\boldsymbol{L}^{ref} = \boldsymbol{0}_{3\times 1}, \quad (29)$$

where $K_p$ is a feedback gain which compensates the error caused by time derivative of Jacobian, $\tilde{\boldsymbol{c}}^{ref}$ is the target position of CoM, $\dot{\tilde{\boldsymbol{c}}}^{ref}$ is the target speed of CoM and $z_B$ is the target height of the pelvis. As specified by (28) we made special treatment for the $z$ element of the linear momentum. This is because the constant pelvis height is desirable for most of the case.

Figure 5 shows reference right foot speed $\boldsymbol{\xi}_{F_1}^{ref}$ to obtain the kick motion. Since the left foot stays on the floor we set $\boldsymbol{\xi}_{F_2}^{ref} = 0$ for entire sequence. Substituting those foot speed, $\boldsymbol{P}^{ref}$ and $\boldsymbol{L}^{ref}$ into (10) and using (12), we obtain the body speed and the joint speeds except leg joints. Finally, the leg joint speeds are calculated by (3).

In Fig.3, we set a selection matrix as identity, so that all momentum follows the given reference. The robot starts from the neutral posture, moves its CoM on the left foot(0.0s → 2.0s), swings the right leg back (2.0s → 3.0s), and kicks forward (3.0s → 4.0s). The

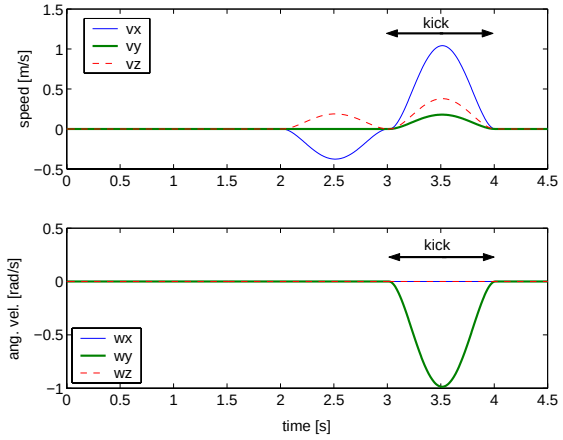


Figure 5: Reference velocity of right foot $\boldsymbol{\xi}_{F_1}^{ref}$

upper graph of Figure 6 shows the corresponding linear momentum during this action. We see $P_y$ increases and decreases from 0.0s to 2.0s which represents the initial motion of the CoM from center to left. $P_z$ have a big change around 3.5s as the result of kick motion and pelvis height control done by (28). The lower graph of the same figure shows the total angular momentum around CoM which is kept around zero as specified in (29). To achieve this, the robot throws back its body when it swings the leg back, and the

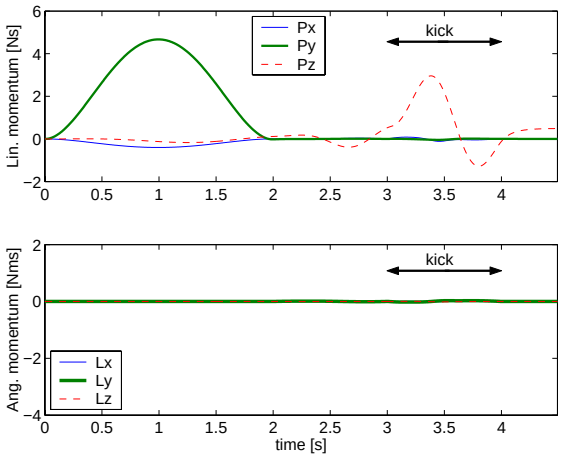


Figure 6: Momentum change during kick action ($S = E$)

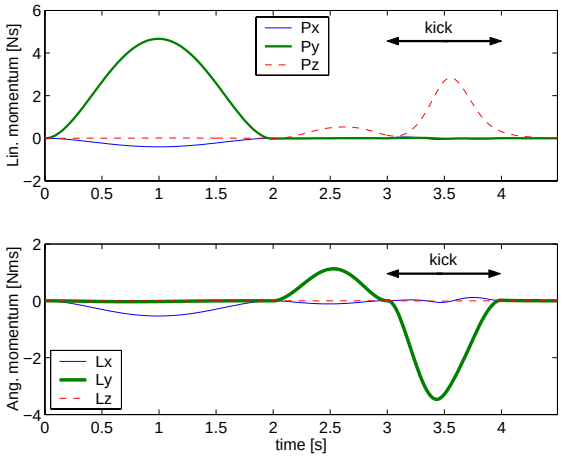


Figure 7: Momentum change during kick action ($S = [\boldsymbol{e}_1\boldsymbol{e}_2\boldsymbol{e}_3\boldsymbol{e}_6]^T$)

robot bends forward when it kicks forward. This motion, however, cannot be realized by the actual robot since the angle of hip pitch joint exceeds the movable range.

To prevent the body swing at kicking, we chose a selection matrix $S = [\boldsymbol{e}_1\boldsymbol{e}_2\boldsymbol{e}_3\boldsymbol{e}_6]^T$ so that the Resolved Momentum Control will not take care of the angular momentum around roll and pitch axes. Figure 4 shows its result. Now we see the kick motion of natural look with upright body posture. Figure 7 shows the corresponding momentum. In the lower graph, we can observe $L_x$ and $L_y$ are no longer kept zero. However, the vertical angular momentum $L_z$ is kept zero which causes natural compensating motion by twisting the waist joint and swinging the arms.

Figure.8 shows experimental result that we gives the same pattern of Fig.4 to HRP-2. The robot could perform kick action with good stability.

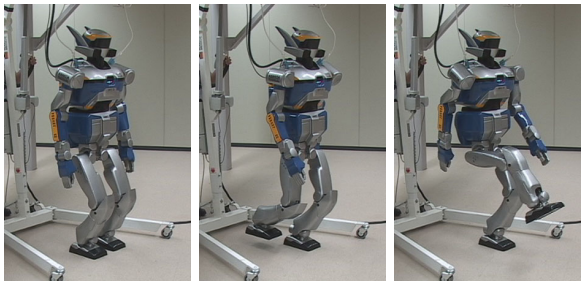

Figure 8: Kick experiment: $S = [\boldsymbol{e}_1\boldsymbol{e}_2\boldsymbol{e}_3\boldsymbol{e}_6]^T$

### 5.2 Walking motion

Figure 9 shows snapshots of the walking experiment. We generated a walking pattern based on the 3D Linear Inverted Pendulum Mode [13]. Giving its ideal pendulum motion as the target position and speed of the CoM, the reference linear momentum was calculated by (27) and (28). As we did in the kick motion, we omitted the control of the angular momentum around roll and pitch axis. As shown in Fig.9, we realized a stable walking motion with natural arm swing. The Zero-Moment Point (ZMP) and the projected hip motion is shown in Figure 10. Since the ZMP trajectory is kept inside of the support area (shown by dotted lines), we can see a proper motion is generated by the Resolved Momentum Control.

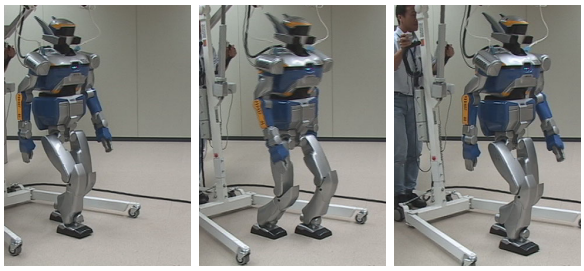

Figure 9: Walk experiment: $S = [\boldsymbol{e}_1\boldsymbol{e}_2\boldsymbol{e}_3\boldsymbol{e}_6]^T$

## 6 Conclusions

We proposed the Resolved Momentum Control which is a method to generate a robot motion with

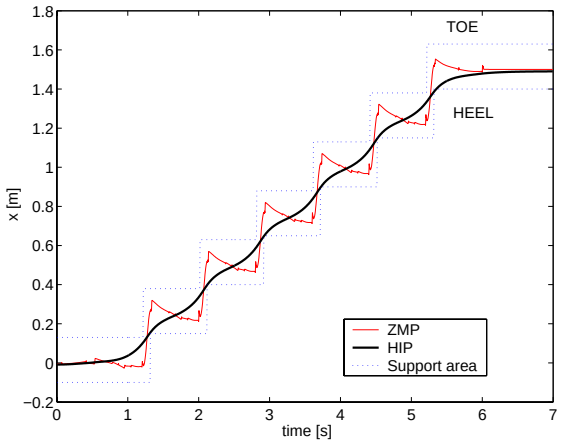


Figure 10: Hip motion and Zero-moment point (simulation)

given linear/angular momenta. We demonstrated its application for balancing and walking by using the humanoid robot HRP-2. We also applied it to the different humanoid robot HRP-1S and it will be reported by Neo et.al [15]. Another application of the Resolved Momentum Control is to generate a hopping and running motion by controlling the vertical element of the linear momentum [14].

The application of the Resolved Momentum Control is not limited in humanoid robotics. As we discussed in Section 3.3, it can be applied to space robots. Moreover, we believe it can be extended for any kind of mobile robots which dynamically interact with environments and propel themselves. Such unified theory for general mobile robots might be an exciting future target.

## Acknowledgments

This research was supported by the Humanoid Robotics Project of the Ministry of Economy, Trade and Industry, through the Manufacturing Science and Technology Center.

## References

[1] Hirai, K., Hirose, M., Haikawa, Y. and Takenaka, T., "The Development of Honda Humanoid Robot," Proc. of the 1998 ICRA, pp.1321–1326, 1998.

[2] Pratt, J. and Pratt, G., "Intuitive Control of a Planar Bipedal Walking Robot," Proc. of the 1998 ICRA, pp.2014–2021, 1998.

[3] Nishiwaki, K., Sugihara, T., Kagami, S., Kanehiro, F., Inaba, M., and Inoue, H., "Design and Development of Research Platform for Perception-Action Integration in Humanoid Robot: H6," Proc. Int. Conference on Intelligent Robots and Systems, pp.1559–1564, 2000.

[4] Gienger, M., Löffler, K. and Pfeiffer, F., "A Biped Robot that Jogs," Proc. of the 2000 ICRA, pp.3334–3339, 2000.

[5] Kaneko, K., Kanehiro, F., Kajita, S., Yokoyama, K., Akachi, K., Kawasaki, T., Ota, S. and Isozumi, T., "Design of Prototype Humanoid Robotics Platform for HRP," Proc. of IROS 2002, 2002.

[6] Wooten,W.L and Hodgins, J.K., "Simulating Leaping, Tumbling, Landing and Balancing Humans," Proc. of 2000 ICRA, pp.656-662, 2000.

[7] Kagami, S., Kanehiro, F., Tamiya, Y., Inaba, M., and Inoue, H., "AutoBalancer: An Online Dynamic Balance Compensation Scheme for Humanoid Robots," Proc. of the 4th Inter. Workshop on Algorithmic Foundation on Robotics (WAFR'00), 2000.

[8] Sugihara,T., Nakamura,Y. and Inoue, H.: Realtime Humanoid Motion Generation through ZMP Manipulation based on Inverted Pendulum Control, Proc. of ICRA 2002, pp.1404-1409, 2002.

[9] Baerlocher,P. and Boulic, R., "Task-Priority Formulations for the Kinematic Control of Highly Redundant Articulated Structures," Proc. of 1998 IROS, pp.323-329, 1998.

[10] Umetani, Y. and Yoshida, K, "Resolved Motion Rate Control of Space Manipulators with Generalized Jacobian Matrix," IEEE Trans. on Robotics and Automation, Vol.5, No.3, pp.303-314, 1989.

[11] http://www.kawada.co.jp/ams/promet/index_e.html, 2003.

[12] Inoue,H., Tachi,S., Nakamura,Y., Hirai,K., Ohyu,N., Hirai,S., Tanie,K., Yokoi,K. and Hirukawa,H., Overview of Humanoid Robotics Project of METI, *Proc. of the 32nd ISR*, April, 2001.

[13] Kajita,S., Kanehiro,F., Kaneko,K., et.al: The 3D Linear Inverted Pendulum Mode: A simple modeling for a biped walking pattern generation, Proc. of 2001 IROS, pp.239-246, 2001.

[14] Nagasaki,T., Kajita,S., Yokoi,K., Kaneko,K. and Tanie,K., "Running Pattern Generation and Its Evaluation Using A Realistic Humanoid Model," Proc. of 2003 ICRA, 2003.

[15] Neo E.S., Yokoi, K., Kajita, S. and Tanie K. "A Method of Teleoperating a Humanoid Robot Integrating Operator's Intention and Robot's Autonomy – An Experimental Verification –," Proc. of 2003 IROS, 2003.